ELSEVIER

Journal of Photochemistry and Photobiology A: Chemistry 93 (1996) 199–203

Journal of PHOTOCHEMISTRY AND PHOTOBIOLOGY A:CHEMISTRY

Application of concept of relative photonic efficiencies and surface characterization of a new titania photocatalyst designed for environmental remediation

Halima Tahiri [a], Nick Serpone [a,*], Raymond Le van Mao [b]

[a] *Laboratory of Pure and Applied Studies in Catalysis, Environment and Materials, Department of Chemistry and Biochemistry, Concordia University, Montreal, Que. H3G 1M8, Canada*

[b] *Catalysis Laboratory, Department of Chemistry and Biochemistry, Concordia University, Montreal, Que. H3G 1M8, Canada*

Received 23 June 1995; accepted 11 August 1995

Abstract

The relative photonic efficiency ζ_r for the TiO_2 photocatalyzed transformation and mineralization of phenol (standard process and product) has been determined for a new industrially available TiO_2 specimen. Under otherwise identical conditions of catalyst loading, pH, phenol concentration and temperature (ambient) the Hombikat UV-100 specimen was approximately four times less efficient than the Degussa P-25 analog (standard photocatalyst). The new titania material was also characterized by X-ray powder diffraction and by nitrogen adsorption–desorption isotherms at liquid nitrogen temperature. The sample is porous with mesopores of about 5.6 nm (diameter) and the Brunauer–Emmett–Teller surface area is 189 $m^2\ g^{-1}$. X-ray powder patterns confirm the anatase structure of the UV-100 sample.

Keywords: Relative photonic efficiencies; Heterogeneous photocatalysis; Titania photocatalysis; Surface characterization; Environmental remediation

1. Introduction

A description of quantum yields Φ, which provide a means of comparing two or more photochemical or photophysical events, poses few problems in homogeneous photochemistry. By contrast, a similar description in heterogeneous photochemistry is further complicated by such fundamental unknown quantities as (a) the extent of light absorption by the chromophore particulates rendered difficult by the often significant extent of light scattering, (b) the different textural properties of the surface of particles, (c) the variety of events occurring during a heterogeneous photocatalytic process and (d) not least the nature of the solid–solution interface.

In two earlier paper [1,2] we described a method by which the relative photonic efficiencies ζ_r of photocatalytic processes could be obtained, which avoided the question of how many photons are absorbed by the active photocatalyst and which attenuated other unknowns by carrying out the experiments under otherwise identical conditions. The method permits a comparison of various photocatalytic processes and determination of which photocatalyst is the more suitable and more efficient for a given process and for a given organic substrate to be mineralized. The present work reports on the latter issue. It should be noted that these relative photonic efficiencies can subsequently be converted to quantum yields once a precise Φ for standard product and standard process not yet chosen has been obtained by utilizing less facile, more complex procedures [3].

Specifically, we address the efficiency of a relatively new, industrially available titania material (commercialized for environmental remediation) for a given photomineralization process: phenol degradation to carbon dioxide. Two materials were examined: (i) Degussa P-25 titania and (ii) Hombikat UV-100 titania with the former used as the standard photocatalyst [2].

2. Experimental section

Degussa P-25 titania was a kind gift from Degussa Canada Ltd., and the Hombikat UV-100 specimen was generously donated by Sachtleben Chemie GmbH, Germany. Other chemical products were of reagent grade quality and were used without further treatment. The two titania samples were also used as received from the suppliers; their respective properties as given by the manufacturers are presented

* Corresponding author.

SSDI 1010-6030(95)04195-8

Table 1
Physicochemical data of the two titania specimens examined

Property	Degussa P-25 TiO_2[a]	Hombikat UV-100 TiO_2[b]
Physical state	White powder	White powder
Composition (%)	≈80 anatase, ≈20 rutile	100 anatase [b,c]
Density (g cm^{-3})	3.8	3.9
BET surface area (m^2 g^{-1})	≈55	>250 (189)[c]
Average primary particle size (nm)	≈30	<10
pH in aqueous solution	3–4	≈6
Contents		
SiO_2 (%)	<0.2	–
Al_2O_3 (%)	<0.3	–
Fe_2O_3 (%)	<0.01	–
TiO_2 (%)	>97	>99
HCl (%)	<0.3	–
Calcining losses (%)	<2 (1000 °C)	9 (850 °C)
Porosity	Non-porous	Porous [c] (mesopores, about 5.6 mm in diameter)
Volatiles (%)	–	8 (105 °C)

[a] [4].
[b] [5].
[c] This work.

in Table 1 [4,5]. The water was deionized and doubly distilled.

The photocatalytic procedures and chemical analyses of accessible intermediates and final product were carried out almost identically with those reported elsewhere [2]. Powder X-ray diffraction patterns of the UV-100 specimen were obtained with a Philips PW1050-25 diffractometer using Ni-filtered Kα radiation of copper ($\lambda = 1.5417$ Å). High performance liquid chromatography (HPLC) analyses were done on a Waters Associates liquid chromatograph (501 pump; 441 absorbance detector; 3.9 mm × 300 mm reverse phase C-18 μ-Bondapak™) coupled to an HP-3396A integrator. Total organic carbon analyses were carried out on a Shimadzu TOC-500 analyzer.

The textural properties of the solid Hombikat UV-100 were examined by nitrogen adsorption–desorption techniques using a Micromeretics ASAP 2000 instrument. It permitted a study of the isotherms of nitrogen adsorption–desorption at liquid-nitrogen temperature and the determination (i) of the Brunauer–Emmett–Teller (BET) surface area [6] and (ii) the Barrett–Joyner–Halenda desorption average pore size [7]. In this regard, we note that micropores, mesopores and macropores correspond to pore diameters in the 0–2 nm, 2–50 nm and above 50 nm regions respectively according to the recent classification proposed by IUPAC [8].

3. Results and discussion

Titania in all its forms (rutile, anatase, brookite and amorphous) is non-toxic [5] and useful in various industrial and commercial applications (e.g. the paint industry, cosmetics and medicinal fields) and of importance in the present context in the area of environmental detoxification as an excellent photocatalytic material to mineralize a variety of organic pollutants by photo-oxidation and to dispose of different metallic cations and complexes by photoreduction [9]. Both redox chemistries are simultaneously responsive on a TiO_2 particulate surface. To the extent that these redox chemistries must necessarily take place at the solid–solution interface [10,11], different materials will necessarily possess different characteristic surface properties (e.g. density of lattice and surface traps, and impurities) dependent on the mode of preparation, all of which are expected to affect the interfacial dynamics strongly and thus the process efficiencies. These have posed a difficult problem to the chemist or researcher to establish a protocol by which comparisons between processes and between different available materials could be made. The concept of relative photonic efficiencies provides a useful protocol.

The prime characteristic differences between the Degussa P-25 titania specimen and the Hombikat UV-100 analogue are their composition (mixed anatase–rutile phases and completely anatase respectively), their BET surface area (about four times greater in the UV-100 specimen), and their porosity (non-porous and porous respectively). These and other physicochemical features are summarized in Table 1. Fig. 1 which illustrates the adsorption–desorption isotherms of nitrogen indicates that the Hombikat material has no micropores. This is confirmed by the BET and volume sorption data normally associated with the micropores, non-existent in this specimen. Rather, the shape of the hysteresis loop in Fig. 1 suggests the presence of mesopores, in accord with the value of the average pore size of about 5.6 nm (Table 1).

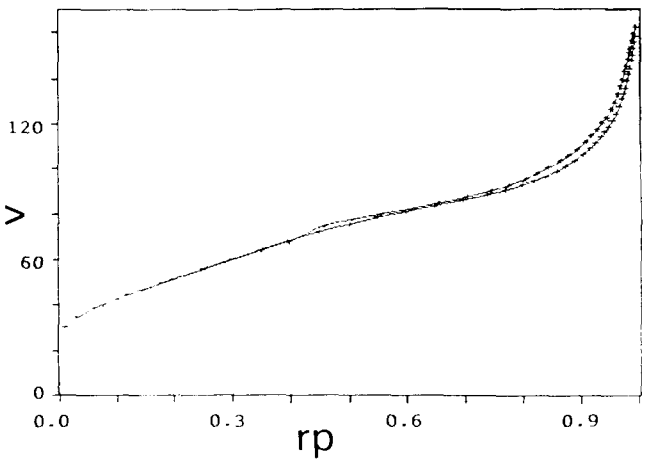

Fig. 1. Isotherms of nitrogen adsorption–desorption: V, volume of nitrogen adsorbed ($cm^3\ g^{-1}$); rp, relative pressure (P/P_0).

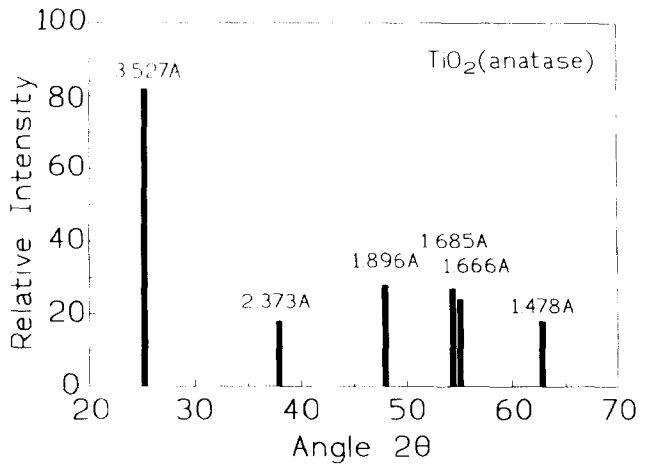

Fig. 2. X-ray powder diffraction pattern for the Hombikat UV-100 specimen. The numbers in the figure correspond to the d spacings for the anatase structure of TiO_2.

The total porosity calculated for this material is about 0.265 $cm^3\ g^{-1}$. By contrast the P-25 specimen is non-porous.

Fig. 2 illustrates the X-ray powder pattern for the Hombikat UV-100 titania specimen and confirms the manufacturer's report [5] that the only crystalline phase present is that of anatase. However, BET surface area measurements indicate a value lower than reported (189 $m^2\ g^{-1}$ vs. greater than 250 $m^2\ g^{-1}$) for this porous specimen. The presence of mesopores could influence process efficiency.

3.1. Photodegradation of phenol

We continue to use phenol as our standard product and its photomineralization as the standard process [2] in comparing process efficiencies. Irradiation of TiO_2 generates conduction band electrons and valence band holes both of which are rapidly trapped in less than 1–10 ps [11] as Ti^{3+} centers for the trapped electrons and as $\equiv Ti–^{\bullet}OH$ for the trapped holes respectively. It is these surface-trapped carriers that ultimately lead to the observed photoredox chemistries in competition with various photochemical and photophysical events; quantum efficiencies will be less than about 0.10 [11]. In air-equilibrated aqueous media, molecular oxygen intercepts the photoelectrons to give superoxide radical anions which some workers [12] have suggested are the principal entity to produce tetroxides and consequently photo-oxidized products. This view, however, is not universally shared [9] although the essential role of molecular O_2 (and H_2O) was first recognized by some of us nearly a decade ago [13].

Fig. 3 depicts the results for the standard Degussa P-25 TiO_2 specimen. The disappearance of phenol in a suitably irradiated (wavelengths below 400 nm) aqueous titania suspension (pH ≈ 3) takes place by apparent first-order kinetics: $k_{app} = 0.033 \pm 0.002\ min^{-1}$. Under the conditions used, we observe only formation of hydroquinone as the only hydroxylated aromatic intermediate (as also reported earlier [2]). A mass balance exercise suggests that other intermediates do form but were intractable by our analytical methods (Fig. 3, dotted curve and full squares).

The results of the photomineralization of phenol with the Hombikat UV-100 titania are indicated in Fig. 4. Phenol also disappears via apparent first-order kinetics ($k_{app} = 0.013 \pm 0.001\ min^{-1}$). Two hydroxylated phenyl intermediates were identified: hydroquinone and catechol in nearly equal amounts and under conditions identical with those used for the Degussa sample (see above); similar observations were made earlier [2] for a titania specimen obtained from Sargent–Welch. This calls attention to and confirms the notion that the nature of the solid–solution interface influences the temporal course of the oxidative photomineralization. It is not surprising then that process efficiencies also

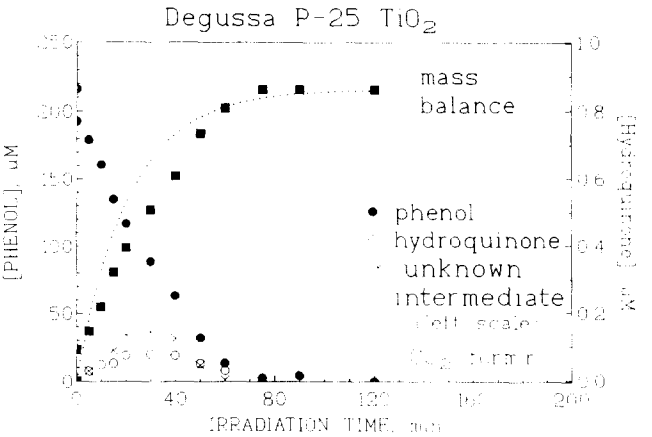

Fig. 3. Plots showing the disappearance of phenol (●) (216 μM; pH ≈ 3; $k = 0.033 \pm 0.002\ min^{-1}$) against irradiation time, together with the formation and decay of hydroquinone (○) in aqueous suspensions of Degussa P-25 TiO_2: ■, mass balance equal to $\{[phenol]_0 - ([phenol + hydroquinone]_t\}$ where $[phenol]_0$ is the initial concentration of phenol; ·····, curve drawn using the rate of disappearance of the total organic carbon (see Fig. 5; $0.047 \pm 0.003\ min^{-1}$ for mineralization of phenol); ×, difference between the dotted curve and the data shown as full squares which we take to be some unknown intermediate or intermediates formed in the photomineralization process.

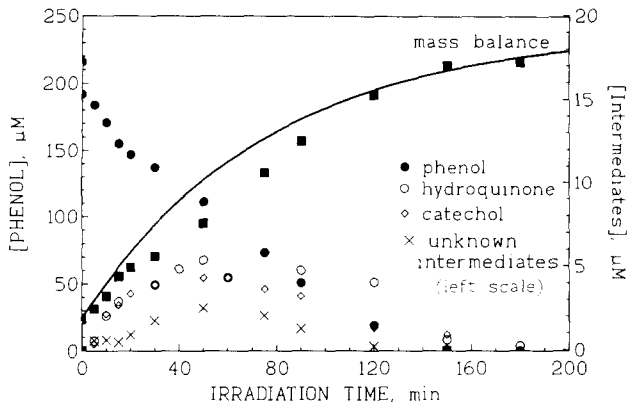

Fig. 4. Graph illustrating the photocatalyzed disappearance of phenol (●) (216 μM; pH ≈ 3; $k = 0.015 \pm 0.001$ min^{-1}) in the presence of irradiated Hombikat UV-100 TiO_2 specimen, together with the formation and decay of the intermediates hydroquinone (○) and catechol (◇); ■, difference between the initial phenol concentration $[phenol]_0$ and $[phenol + hydroquinone + catechol]_t$; —, curve for the mineralization of phenol drawn using the rate of disappearance of the total organic carbon (see Fig. 5; $k = 0.013 \pm 0.001$ min^{-1} for mineralization of phenol); ×, difference between the full curve and the full squares for some unknown intermediate or intermediates.

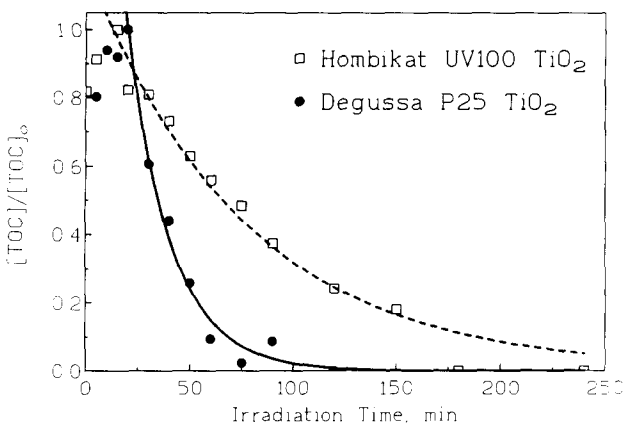

Fig. 5. Plots illustrating the first-order disappearance of the total organic carbon from the aqueous phenolic solutions containing Degussa P-25 (●) and Hombikat UV-100 (□) titania samples. Note the brief induction period before the first order process initiates.

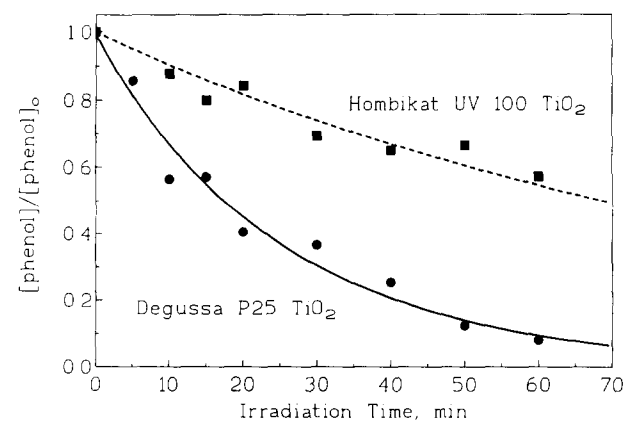

Fig. 6. Photodegradation of phenol during the first half-life for the Hombikat and for the first three half-lives for the Degussa titania (conditions nearly the same as those of Figs. 3 and 4).

differ and depend on the photocatalyst source and method of preparation. The mass balance exercise (as done above; also see caption to Figs. 3 and 4 for details) shows that one or more additional intermediates form which we were unable to identify.

The disappearance of total organic carbon from the aqueous suspensions is illustrated in Fig. 5 for the titania specimens. Both show an induction period of about 20 min following irradiation, after which the total organic carbon is transformed into CO_2 via first-order kinetics: $k_{TOC} = 0.047 \pm 0.003$ min^{-1} and $k_{TOC} = 0.013 \pm 0.001$ min^{-1} for Degussa P-25 and Hombikat UV-100 respectively; quantitative photomineralization of phenol is achieved in about 1.5–2 h with Degussa P-25 and in approximately 4–5 h with Hombikat UV-100 titania.

3.2. Relative photonic efficiencies

In an experiment design to assess process efficiencies by the ζ_r method, phenol disappearance was monitored more frequently during the early stages (the method protocol suggested earlier [2] used initial rates). The results are shown in Fig. 6; k_{app} are 0.039 ± 0.003 min^{-1} and 0.010 ± 0.001 min^{-1} respectively. Consequently, the relative photonic efficiency for the Hombikat UV-100 specimen is $\zeta_r = 0.25 \pm 0.03$ (relative to Degussa's titania as the standard photocatalyst [2]). A similar inference can be made by the fundamentally more important TOC degradation process in any environmental remediation application; estimates from respective first-order rates yield $\zeta_r \approx 0.27 \pm 0.03$.

4. Final remarks

Additional data were obtained on the recently commercially available Hombikat UV-100 titania; some of the earlier assertions have been confirmed. Using the photo-oxidative degradation of phenol as the standard process and phenol as the standard product against which to estimate process efficiencies, the Hombikat specimen appears less efficient than the corresponding Degussa P-25 by a factor of about 4. When ζ_r is measured against the photomineralization of another product (e.g. degradation of dichloroacetic acid), the Hombikat specimen might prove to be more efficient (see for example [14]). This recalls the notion that, once the photochemical and photophysical events have taken place in the lattice and on the photocatalyst surface, photo-oxidations will proceed along a path germane and specific to the substrate being oxidized and which may ultimately dictate the kinetics of degradation.

Acknowledgements

This work was supported in part by the Natural Sciences and Engineering Research Council of Canada, by a Collab-

orative Exchange Grant in the France-Quebec Programme de Cooperation, and by a NATO collaborative grant (CRG 890746). One of us (N.S.) thanks Dr. P. Pichat for his kind hospitality during a Mission de Recherche – June 1995 to the Ecole Centrale Lyon as part of the France-Quebec programme. H.T. was a visiting researcher from the Ecole Centrale de Lyon during 1994–1995.

References

[1] N. Serpone, R. Terzian, D. Lawless, P. Kennepohl and G. Sauve, *J. Photochem. Photobiol. A: Chem., 73* (1993) 11.
[2] N. Serpone, G. Sauve, R. Kohl, H. Tahiri, P. Pichat, P. Piccinini and E. Pelizzetti, *J. Photochem. Photobiol. A: Chem.*, in press.
[3] L. Sun and J.R. Bolton, *J. Phys. Chem.*, submitted for publication.
[4] *Bull. 56,* Degussa Canada Ltd., Burlington, Ontario, Canada.
[5] *Hombikat UV-100 Bull.*, Sachtleben Chemie GmbH, PO Box 17 04 54, D-47184 Duisburg, Germany, 24 June 1994.
[6] S. Brunauer, P.H. Emmett and E. Teller, *J. Am. Chem. Soc., 60* (1938) 309.
[7] E.P. Barrett, L.G. Joyner and P.P. Halenda, *J. Am. Chem. Soc., 73* (1951) 373.
[8] K.S. Sing, D.H. Everett, R.A.W. Haul, L. Moscou, R.A. Pierotti, J. Rouquerol and T. Siemienewska, *Pure Appl. Chem., 57* (1985) 603.
[9] N. Serpone, *Res. Chem. Intermed., 20* (1994) 953.
[10] G. Rothenberger, J. Moser, M. Gratzel, N. Serpone and D.K. Sharma, *J. Am. Chem. Soc., 107* (1985) 8054.
[11] N. Serpone, D. Lawless, R. Khairutdinov and E. Pelizzetti, *J. Phys. Chem.*, in press.
[12] A. Heller, *Acc. Chem. Res.*, in press.
[13] M. Barbeni, E. Pramauro, E. Pelizzetti, E. Borgarello, M. Gratzel and N. Serpone, *Nouv. J. Chim., 8* (1984) 547.
[14] D.W. Bahnemann, quoted in [5].